

Supplementary Information

Effect of $\text{CH}_3\text{NH}_3\text{PbI}_3$ Thickness on Device Efficiency in Planar Heterojunction Perovskite Solar Cells

Dianyi Liu, Mahesh K. Gangishetty and Timothy L. Kelly*

Department of Chemistry, University of Saskatchewan
110 Science Place, Saskatoon, SK, Canada, S7N 5C9

* e-mail: tim.kelly@usask.ca

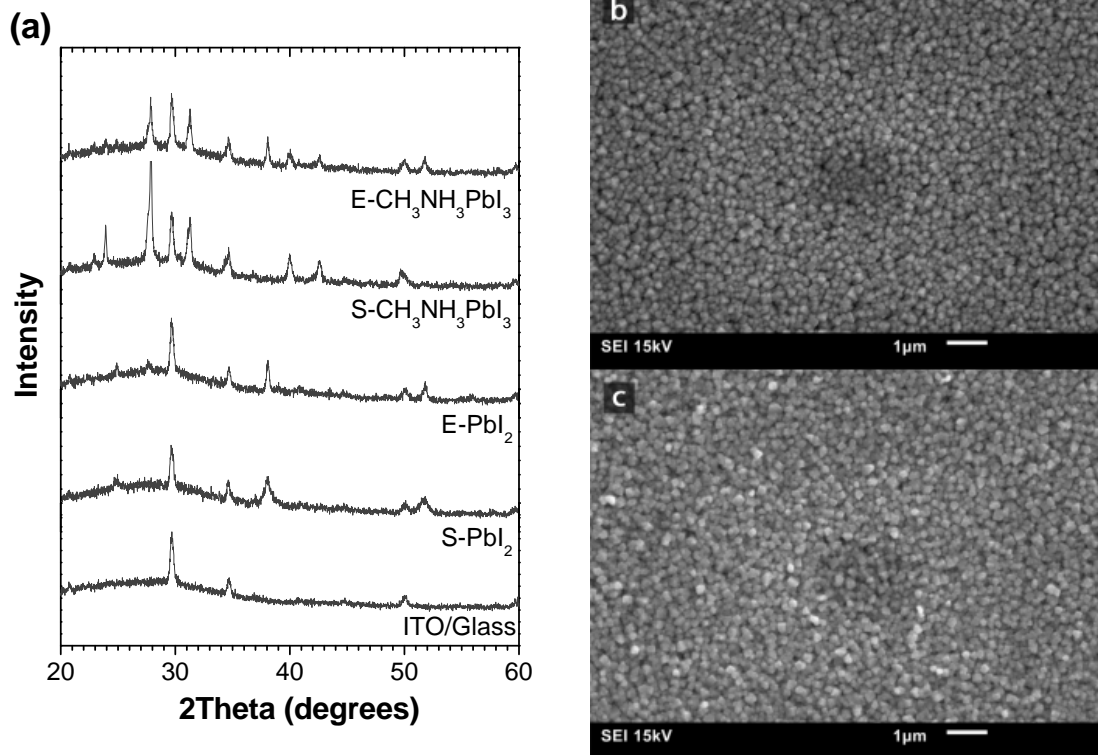
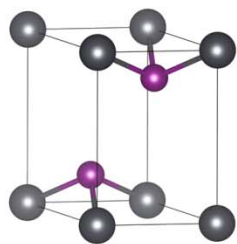
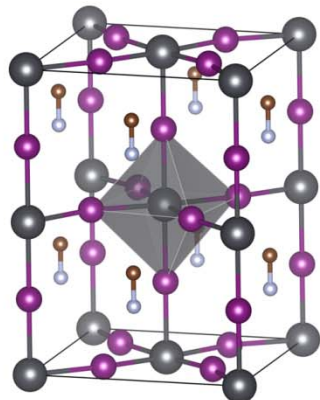
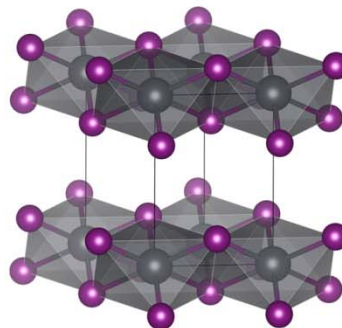


Figure S1. (a) Powder X-ray diffraction patterns of PbI₂ films deposited by spin coating (S-PbI₂) and thermal evaporation (E-PbI₂), and the corresponding CH₃NH₃PbI₃ films after dipping in methylammonium iodide solution. All films were deposited on ITO/glass substrates. (b) SEM micrograph of a perovskite film produced from a spin coated PbI₂ film; (c) SEM micrograph of a perovskite film produced from an evaporated PbI₂ film.



Lead iodide
Cell Volume = 124 \AA^3



Tetragonal $\text{CH}_3\text{NH}_3\text{PbI}_3$
Cell Volume = 990 \AA^3

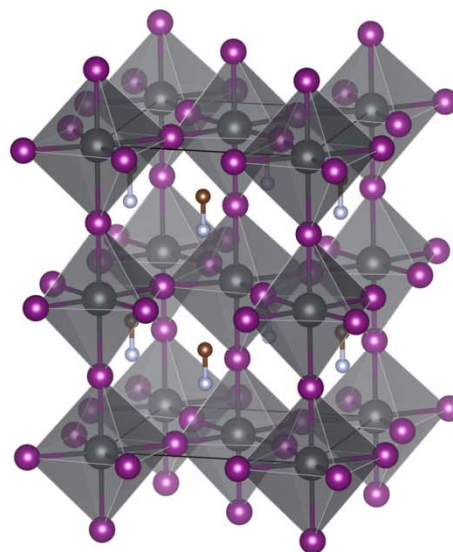


Figure S2. The unit cells and cell volumes of lead iodide and tetragonal $\text{CH}_3\text{NH}_3\text{PbI}_3$: Pb (grey), I (purple), C (brown) and N (pale blue). The unit cell of $\text{CH}_3\text{NH}_3\text{PbI}_3$ contains four $\text{CH}_3\text{NH}_3\text{PbI}_3$ units, and so the volume per $\text{CH}_3\text{NH}_3\text{PbI}_3$ repeat unit is 248 \AA^3 .

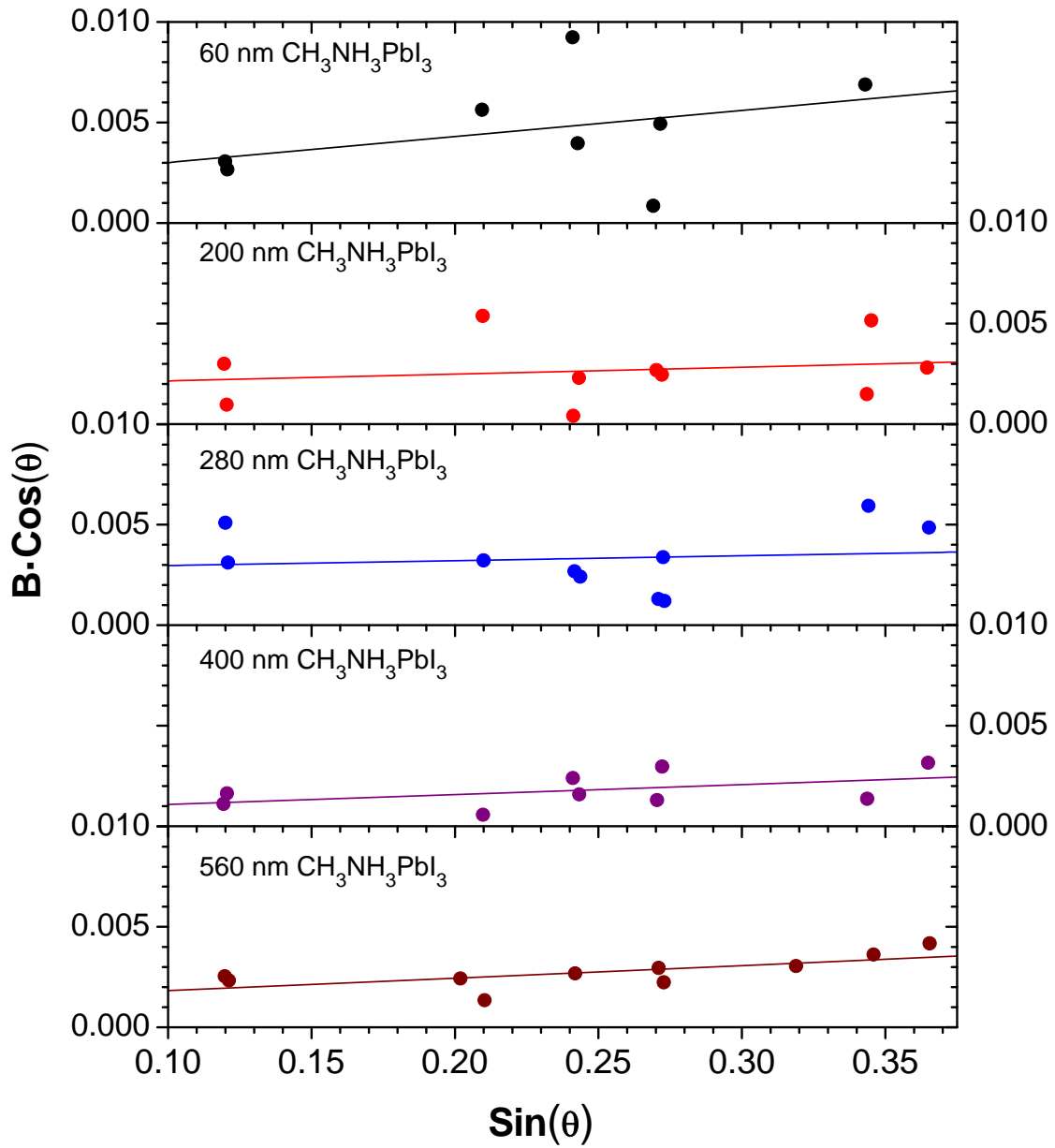


Figure S3. Williamson-Hall plots for $\text{CH}_3\text{NH}_3\text{PbI}_3$ films of various thicknesses. Contributions from instrumental broadening were not subtracted from the data; however, the FWHM of a polycrystalline Si standard indicated the degree of instrumental broadening to be $< 0.05^\circ$ (2θ).

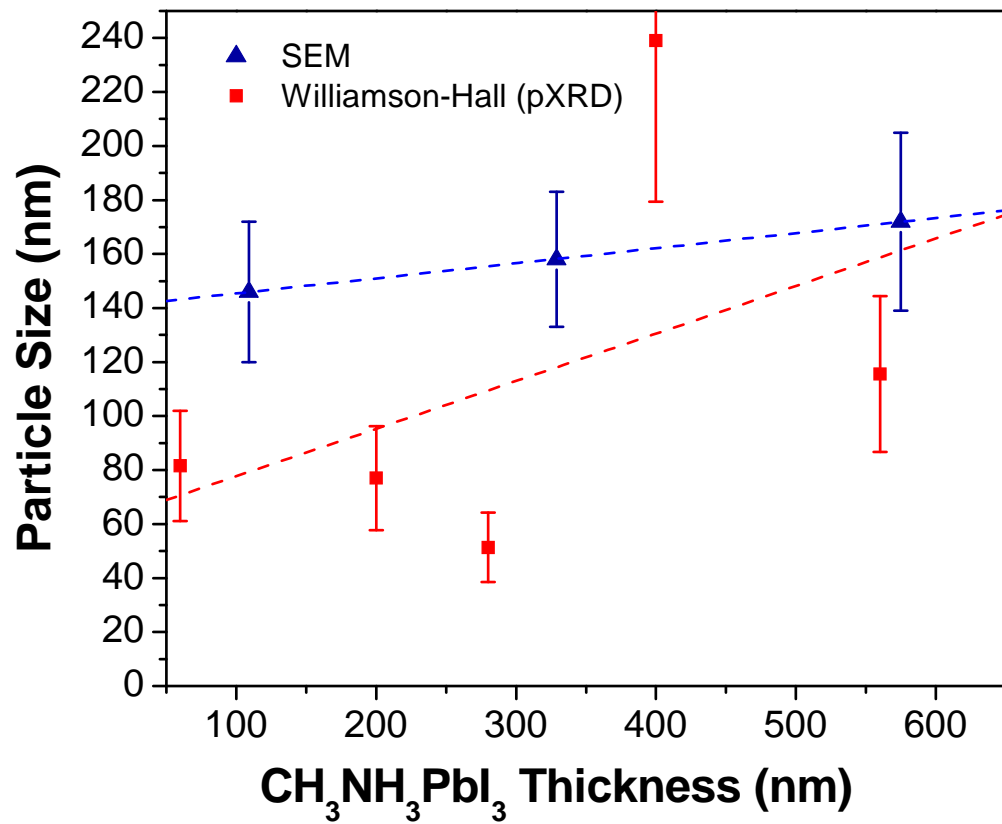


Figure S4. Particle size as measured by SEM (blue triangles) and minimum grain size as determined by a Williamson-Hall analysis of powder X-ray diffraction data (red squares) as a function of perovskite layer thickness. The linear fits are a guide to the eye.

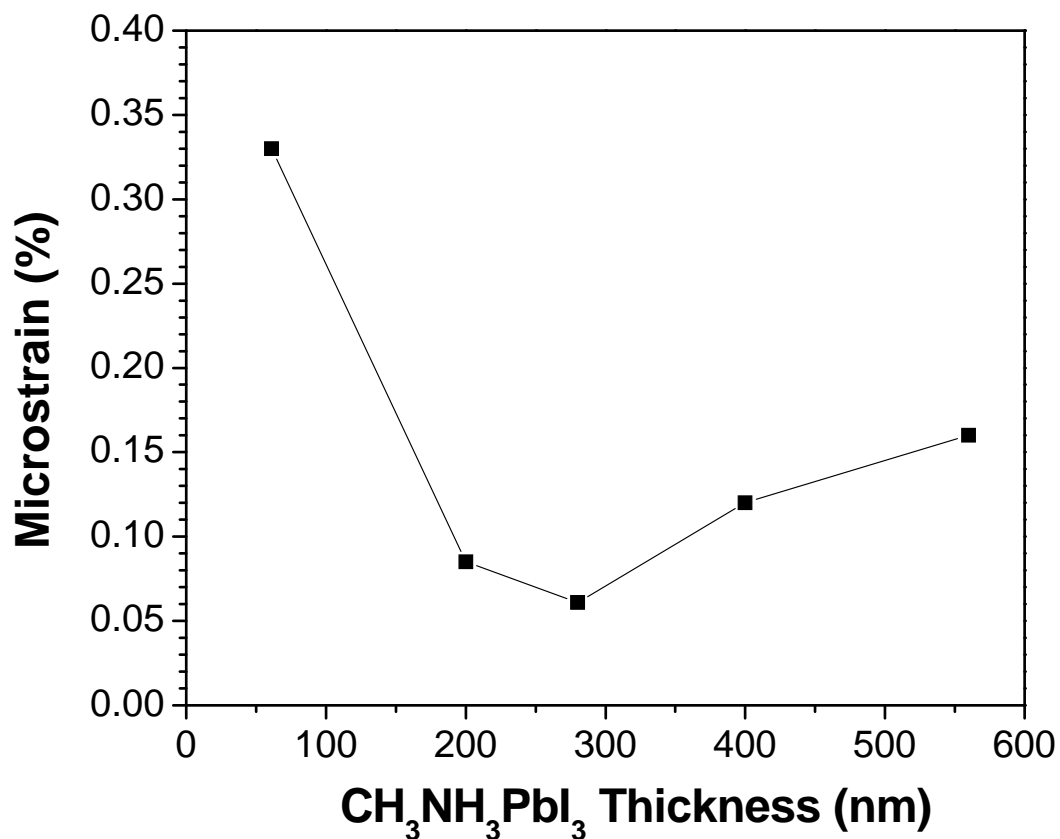


Figure S5. Microstrain (as calculated by a Williamson-Hall analysis of powder X-ray diffraction data) as a function of perovskite layer thickness.

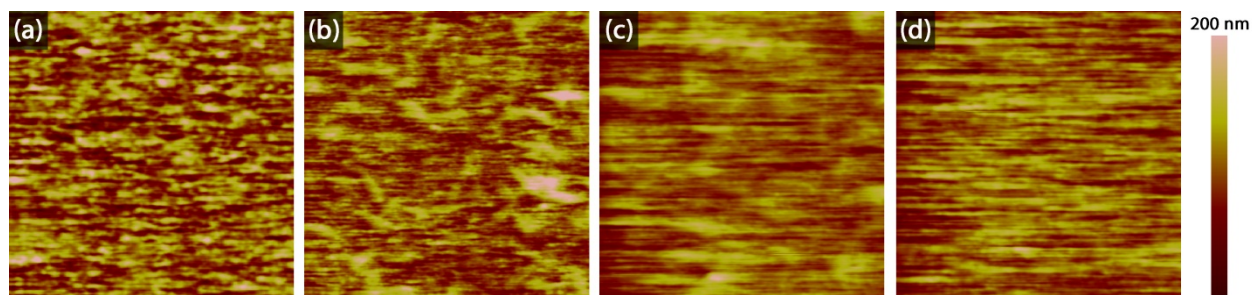


Figure S6. Height mode AFM images of $\text{CH}_3\text{NH}_3\text{PbI}_3$ films of various thicknesses on ITO/ZnO substrates: (a) 200 nm, (b) 280 nm, (c) 400 nm, and (d) 560 nm. All images were of a $15\ \mu\text{m} \times 15\ \mu\text{m}$ area. The samples had root-mean-squared surface roughnesses (R_{rms}) of: (a) 33, (b) 29, (c) 23, and (d) 49 nm, respectively.

Table S1. Average series (R_s) and shunt (R_{sh}) resistances for perovskite solar cells.

CH ₃ NH ₃ PbI ₃ Thickness (nm)	R_s ($\Omega \cdot \text{cm}^2$)	R_{sh} ($\text{k}\Omega \cdot \text{cm}^2$)
110	170	0.22
210	13	3.0
330	8.0	4.0
410	12	0.42
490	41	0.24
580	110	1.2

Table S2. Tabulated fit parameters for the EIS data.

CH ₃ NH ₃ PbI ₃ Thickness (nm)	R_s (Ω)	R_{co} (Ω)	C_{co} (F)	R_{rec} (Ω)	$CPE_{\mu-T}$ (F)	$CPE_{\mu-P}$
110	64	5	1×10^{-7}	1	2×10^{-3}	0.57
330	52	31	6×10^{-3}	116	9×10^{-8}	0.84
580	39	1250	2×10^{-7}	1323	9×10^{-7}	0.67

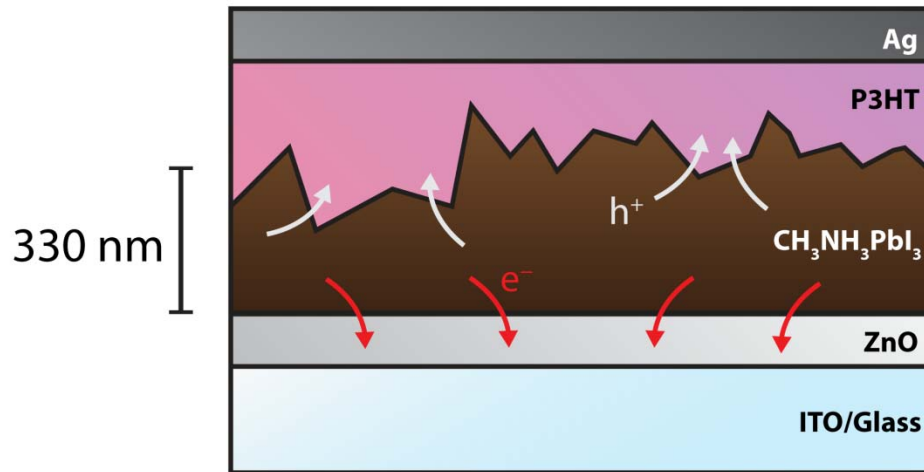


Figure S7. Schematic of the ITO/ZnO/CH₃NH₃PbI₃/P3HT/Ag devices tested in this work, showing the effect of the roughened CH₃NH₃PbI₃/P3HT interface on the hole-extraction efficiency.